Solute Flux Coupling in a Homopore Membrane

JOHN T. VAN BRUGGEN, JUNE D. BOYETT,
ANTONIA L. van BUEREN, and WILLIAM. R. GALEY

From the Department of Biochemistry, University of Oregon Medical School, Portland, Oregon 97201 and the Department of Physiology, University of New Mexico School of Medicine, Albuquerque, New Mexico 87106

ABSTRACT   Our previous studies on solute drag on frog skin and synthetic heteropore membranes have been extended to a synthetic homopore membrane. The 150-Å radius pores of this membrane are formed by irradiation and etching of polycarbonate films. The membrane is 6-μm thick and it has 6×10^8 pores cm^{-2}. In this study, sucrose has been used as the driver solute with bulk flow blocked by hydrostatic pressure. As before on heteroporous membranes, the transmembrane asymmetry of tracer solute is dependent on the concentration of the driver solute. Tracer sucrose shows no solute drag while maltotriose shows appreciable solute drag at 1.5 M sucrose. With tracer inulin and dextran, solute drag is detectable at 0.5 M sucrose. These results are in keeping with the previous findings on heteropore membranes. Transmembrane solute drag is the result of kinetic and frictional interaction of the driver and tracer solutes as the driver flows down its concentration gradient. The magnitude of the tracer flux asymmetry is also dependent on the size of the transmembrane pores.

We have shown in previous papers (1–4) that an asymmetry of transmembrane tracer solute flow can be the result of the interaction or drag that hyperosmotic solute (driver) flow exerts on tracer (driven) solute. These studies which were done on heteroporous, cellulose acetate membranes demonstrated that the magnitude of the interaction depends strongly on driver-tracer molecular size relationships and the pore size of the membrane. The membrane dependence distinguishes our studies from the coupling of solute flows known to take place in free solution (5–7).

The previous studies on heteroporous membranes did not allow for an adequate quantitative treatment of the experimental data. With heteropore membranes, little is known about "pore" size other than the average pore size approximated by the methods of Goldstein and Solomon (8) and Paganelli and Solomon (9). These methods do not provide information on true

pore size distribution, area available for solute flow, length of pore, or the degree of tortuosity of the pore system. With the compressed "brush pile" configuration of cellulose acetate membranes, it may in fact be ambiguous to talk of pores in the classical sense. Because of the structural difficulties of the heteropore membrane, we sought to demonstrate solute drag on a membrane system in which many membrane pore characteristics were rigorously defined. Ideally this would be a right angle, homopore system, for such a system lends itself to a more precise treatment of transmembrane phenomena. A homopore system also may help resolve the question of the role of a postulated circulatory flow in heteropore models (4, 10).

We have been able to demonstrate the solute drag effect of sucrose on a number of solutes on a homopore membrane of 150-Å radius. This drag effect is presented graphically, with equations modified from Kedem and Katchalsky (11–13), and by transmembrane interaction coefficients (13–16).

EXPERIMENTAL

Membrane Preparations

Our initial experiments on homopore membranes were conducted on Nucleopore membrane filters obtained from the General Electric Co., Irradiation Processing Operation, Pleasanton, California. The smallest pore filter then available (2,500-Å radius) did not allow measurable solute interaction because diffusion of small solutes through such large pores resembles that in free solution. The General Electric Co., however, kindly supplied small pieces of experimental membranes with smaller pore sizes and we have studied the solute drag phenomena on a number of these experimental membranes. The present paper contains data obtained on a single membrane preparation having pores of 150-Å radius. Currently, homopore membranes with pore diameter of 80,000 to 300 Å are available from the Nucleopore Corporation, Pleasanton, Calif.

Homopore membranes are formed by the irradiation of polycarbonate films by fission fragments which drill "damage tracks"[1] in the material so exposed (17–20). Etching of the damage tracks with NaOH under controlled conditions of temperature and in the presence of wetting agents provides membranes of measurable size and abundance. These pores are considered to all be right angle but a maximum deviation of 20° from the right angle may be present. Our experimental membranes were studied by C. P. Bean, Margaret Doyle, and E. F. Koch of the Schenectady Laboratories of General Electric. Samples were rotary shadow cast with platinum

---

[1] Key publications in this area have been primarily concerned with studies on membranes made from irradiated mica after etching with HF. This technique was described by Price and Walker (17) and extended by Bean et al. (20), and by Beck and Schultz (21). This porous mica with holes near molecular dimensions can be used without or with a variety of linings for the pores (22).

at an angle of 45° to their surface. Carbon was rotary deposited normal to the shadowed surface and then the direct carbon replicas were dissolved free in methylene chloride. These replicas were then used for transmission micrographs.

In addition to the preformed membranes supplied to us, we carried out extensive studies on membranes irradiated by General Electric and etched in our laboratories. Although excellent solute coupling can be demonstrated on these "homemade" membranes, deviation of theoretical from experimental pore characteristics has caused us to withhold this data in favor of that obtained on the 150-Å membrane cited above. Apparently the controlled etching of the polycarbonate by NaOH requires the presence of special wetting agents and ideal conditions for the formation of true homopore membranes.

Micrographs of the smooth and the rough side of the 150-Å membrane are shown in Fig. 1. The density of holes is determined visually by counting an adequate area of the micrograph, and the pore size is determined by lineal measurement of the micrograph and by diffusion of ^{3}H-water (THO). Table I contains relevant information on characteristics of the homopore membrane.

The theoretical permeability characteristics of the membrane were determined using the following formulations. The dimensionless Reynold's number was calculated from

$$Re = \frac{\rho r^3 \Delta P}{8\eta^2 L}, \tag{1}$$

where ρ is the density of the fluid in gm cm^{-3}, r is radius in centimeters, P is pressure in dynes cm^{-2}, η is viscosity in gm sec^{-1} cm^{-1}, and L is length in centimeters. A value of 5×10^{-7} was found for the membrane indicating that linear, nonturbulent flow was present, thus validating the use of Poiseuille's law.

The theoretical hydraulic permeability for pure water was calculated from Poiseuille's law assuming that the pores are all the same size and that all pores are right angle

$$L_p = n\pi \, d^4 / 128\eta\delta, \tag{2}$$

where n = pore density, d = pore diameter, η = viscosity, and δ = membrane thickness. The calculated or theoretical permeability coefficient (P) for THO was obtained from

$$P_{THO} = n\pi \, d^2 \, D_{THO} / 4\delta, \tag{3}$$

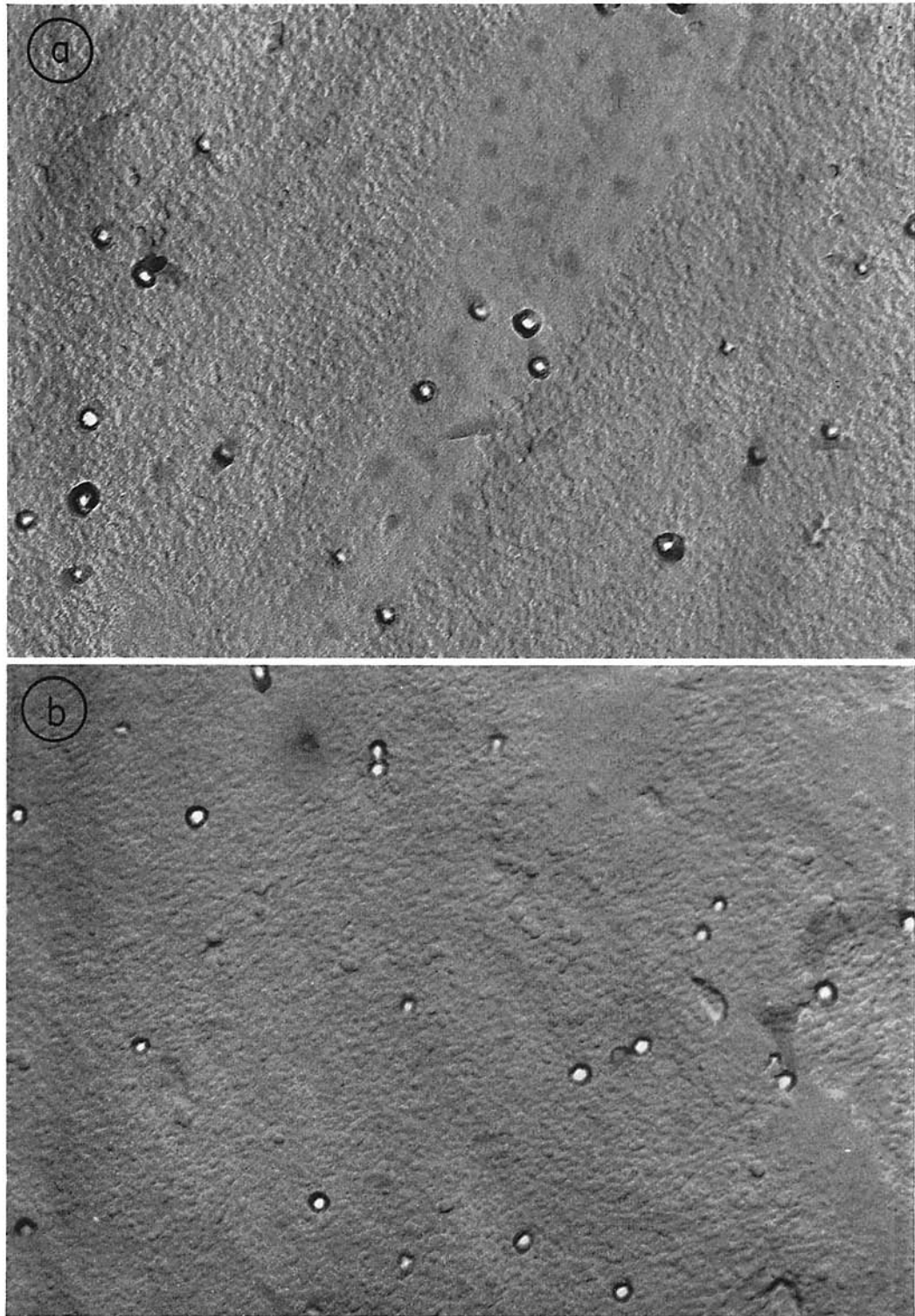where n, d, δ, are as above and D_{THO}, the diffusion coefficient of THO, is

FIGURE 1.   Electron micrograph of homopore membrane no. 118/151 at ×60,000 magnification. (a) Smooth side. (b) Rough side.

2.44×10^{-5} cm^2 s^{-1} (25°C). The experimental L$_p$ was determined by measuring the flow of water due to a hydrostatic pressure gradient across the membrane.

The reflection coefficient, σ, for sucrose was found by determination of the hydrostatic pressure required to block osmotic flow for a known sucrose solution. σ is calculated as

$$\sigma = \pi/\Delta CRT \ (22°C), \tag{4}$$

where π is the osmotic pressure and ΔC the gradient of sucrose across the membrane. The effect of pore size on diffusion was evaluated by the experimental and theoretical ratios D_M/D_o. Beck and Schultz (21) estimated the diffusion hindrance effect by application of the Renkin equation,

$$\frac{D_M}{D_o} = \left(1 - \frac{R_s}{R_P}\right)^2\left(1 - 2.104\frac{R_s}{R_P} + 2.09\left(\frac{R_s}{R_P}\right)^3 - 0.95\left(\frac{R_s}{R_P}\right)^5\right), \tag{5}$$

where D_M/D_o is the ratio of solute diffusivity in the membrane to that in free solution and R_s/R_P is the ratio of solute radius to pore radius.

All tracer flux measurements were made with a zero net volume flow ($J_v = 0$). This condition was obtained by application of hydrostatic pressure as described previously (3, 4). For each sucrose concentration, the hydrostatic pressure required was determined experimentally. All tracer fluxes were measured in steady-state condition after an initial equilibration period.

Consideration of Unstirred Layers

A few comments may be made about the method of mounting the homopore membrane. The area of the membrane used was 8 cm^2. Since a hydrostatic pressure as high as 100-cm H$_2$O was sometimes required to block osmotic water flow and known, constant chamber volumes had to be maintained, rigid support of the membrane was required. This was supplied by 20-mesh stainless steel screens on each side, supported on their edges by a metal ring or cassette (2). All solutions were well stirred by external 600 rpm motors and with a $\frac{1}{4}$-inch Teflon stir bar in each of the $\sim$10-ml chambers.

Because of the potential problem of "unstirred layers," we determined the thickness of these layers by the approach of Ginsburg and Katchalsky (23) which involves comparison of the measured vs. calculated permeabilities of a solute such as THO by the relation:

$$\frac{1}{\omega'} = \frac{1}{\omega} + \frac{2RT}{D}\delta, \tag{6}$$

where ω' is the experimental permeability coefficient, δ is the thickness of the unstirred layer, and D is the diffusion coefficient in free solution. Ginsburg

and Katchalsky found that the effective permeability coefficient for THO changed considerably as the rate of stirring was increased but did not approach a limiting value as it did for other solutes. It must be pointed out that the "rate of stirring" is a condition peculiar to the shape and size of the chamber stirred and the size and pitch of the paddle or bar doing the stirring. In any event, using the equation above, we found the thickness of the unstirred layer to be 30 μm, a value considered to present no major problem in our studies. Also, using locally etched homopore membranes in screened cassettes or mounted free of screen support, we found the theoretical and experimental permeabilities of THO, urea, mannitol, sucrose, and inulin to be identical within the usual limits of error of these measurements.

Experimental Design

In the studies to be described, reference will be made to the direction of tracer movement using the terms influx and outflux. The meaning of these terms is shown in Fig. 2. The hyperosmotic or "driver" solute is shown present on side 2 and the movement of tracer into $(J_T^{1\to2})$ or out of $(J_T^{2\to1})$ being considered as influx and outflux movements. When water or sucrose solutions were present on both sides, the direction of the tracer flux is immaterial and no special notation is used. In practice, tracer fluxes in the two directions were found to be identical when similar solutions bathed the membrane indicating that membrane structural asymmetry did not influence diffusional flow (see Table III).
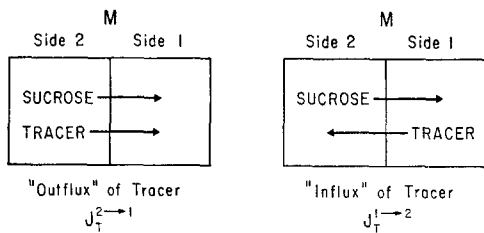

FIGURE 2   FIGURE 3

FIGURE 2.   Schematic model of solute movement. Sucrose, the osmotic or driver solute, is shown on side 2. The tracer solute is shown on side 2 or side 1 to indicate the meaning of "outflux" and "influx" terms. The convention, $J_T^{2\to1}$ indicates the equality of this term with the word outflux.

FIGURE 3.   Method of plotting the P values for a tracer moving in the system in which driver sucrose is present on both sides at a mean ($\bar{C}$) concentration. See text for a detailed explanation of the figure.
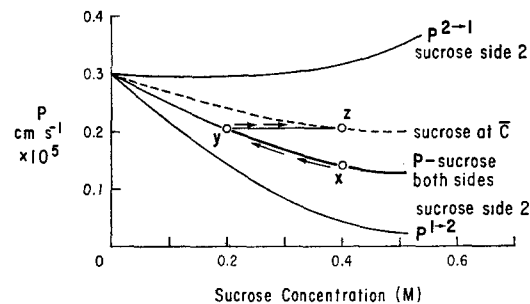
Solutes and Tracers

Sucrose, reagent grade (J. T. Baker Chemical Co., Phillipsburg, N. J.), was used as the hyperosmotic agent. 1-^{14}C-D-mannitol was obtained from Mallinckrodt Chemical Works, St. Louis, Mo. U-^{14}C-sucrose; carboxyl-^{14}C-dextran (MW 16,000–19,000), and ^{3}H-water (THO) were obtained from New England Nuclear, Boston, Mass. Hydroxymethyl-^{14}C-inulin and U-^{14}C-maltotriose were obtained from Amersham/Searle Corp., Arlington Heights, Ill. Reagent grade nonlabeled solute was added to make the tracer solute concentration on the labeled and nonlabeled side 1×10^{-4} M. All solvents and solutions were prefiltered through 0.1-μm Nucleopore filters to aid in preventing plugging of the pores.

Radioassay

100–150-μl aliquots from the diffusion chambers were mixed with 10 ml Aquasol, stabilized with 1 ml H_2O, and were assayed with a Tri-Carb Spectrometer (Packard Instrument Co., Inc., Downers Grove, Ill.). Quenching by the hyperosmolar solute was less than 3% and no correction was made.

RESULTS

The pore size of the membrane (Table I) as shown by EM and P_{THO} methods agrees well with an average pore radius of 150 Å. Bulk water flow measurements (L_p) resulted in a calculated pore size of 178 Å. This larger value is not significantly different from that obtained by EM and P_{THO}. The difference between these calculated values of 150 and 178 reflects the summation of errors of the methodology. The effects of the 150-Å pore size on diffusion can be appreciated by consideration of the theoretical D_M/D_o figures of Table I. It is seen that only a small hindrance to diffusion is expected for mannitol, sucrose, and maltotriose. However, when the ratio of solute and pore sizes approaches 0.1, as with inulin, some hindrance is predicted. In practice, the experimental hindrance for inulin ($D_M/D_o = 0.41$) was greater than that expected from the equation. Hindrance to diffusion does not disturb the solute drag studies which involve bidirectional tracer flows where both flows are equally influenced by solute-pore frictional interaction.

In the present studies, sucrose was used as the driver solute. With this small size solute and with 150-Å pores, it is necessary to increase the sucrose concentration to a high level to demonstrate solute drag. Concomitant with the increase in sucrose concentration from 0 to 1.5 M is an increase in viscosity of the solution from 1.0 to 7.9 (relative to the viscosity of H_2O). Since free diffusion or solute-coupled diffusion is related to the viscosity of the medium, the permeability coefficients of sucrose, maltotriose, inulin, and

dextran were determined at a number of sucrose concentrations. Table II
lists data from these studies where sucrose was present on both sides of the
membrane at the stated concentration. It is clear that the increased con-
centration of the sucrose solution has quite similar effects on the four tracer

TABLE I

DESCRIPTION OF HOMOPORE MEMBRANE NO. 118/151

Structural characteristics	
Pore radius, Å	$155\pm10\%$ (EM)
	$145\pm10\%$ (from P_{THO})
	$178\pm1.5\%$ (from L_p)
Pore density, cm^{-2}	$6.2\pm0.25\%10^8$ (EM)
Pore length, cm	6×10^{-4}
Permeability characteristics	
L_p, cm^3 $dyne^{-1}s^{-1}$	$0.39\pm0.05\times10^{-9}$
σ_{suc}	0.0016

		D_M/D_O		
Diffusion properties	P	Experimental*	Theoretical‡	R_S/R_P
	$cm\ s^{-1}$			
THO	0.16×10^{-3}	1.00	—	—
Mannitol	3.66×10^{-5}	0.88	0.94	0.030
Sucrose	3.12×10^{-5}	0.90	0.92	0.037
Maltotriose	2.29×10^{-5}	0.81	0.91	0.042
Inulin	0.45×10^{-5}	0.41	0.78	0.103
Dextran§	0.55×10^{-5}	—	—	—

* D_M experimental is $P\times$ pore length/pore area, and D_O is the coefficient of diffusion in free
solution.
‡ D_M/D_O theoretical is calculated from the Renkin equation (21). The radius of maltotriose
was assumed to be the same as that of raffinose (6.1 Å).
§ Lack of basic data on molecular shape and diffusion coefficients precludes calculation of dex-
tran values.

TABLE II

EFFECT OF SUCROSE CONCENTRATION ON THE PERMEABILITY
COEFFICIENT OF TRACER SOLUTES WITH SUCROSE ON BOTH SIDES

Sucrose concentration	Viscosity*	Permeability coefficient‡			
		Sucrose	Maltotriose	Inulin	Dextran
M					
0	1.0	3.12 ± 0.15	2.29 ± 0.07	0.45 ± 0.01	0.55 ± 0.02
0.15	1.1	2.50 ± 0.10	—	—	—
0.30	1.3	2.28 ± 0.11	—	—	—
0.50	1.7	2.07 ± 0.08	1.54 ± 0.07	0.37 ± 0.01	0.41 ± 0.04
0.75	2.2	1.35 ± 0.08	—	—	—
1.00	3.1	1.06 ± 0.06	0.65 ± 0.02	0.23 ± 0.01	0.26 ± 0.01
1.50	7.9	0.64 ± 0.03	0.38 ± 0.04	0.10 ± 0.01	0.08 ± 0.01

* Viscosity η relative to water (η/η_{H2O}): From Handbook of Chemistry and Physics, 42nd edi-
tion, Chemical Rubber Co., Cleveland, Ohio, 1960-61, p. 2211.
‡ P in cm $s^{-1}\times10^5\pm1$ SD.

solutes, decreasing the P values in 1.5 molar sucrose to about 20% of their values in water.

Since P values decrease with increasing amounts of sucrose present, it is necessary to use a realistic base of comparison for the results shown in the following figures. In experiments where sucrose is present only on side 2, it is not possible to determine experimentally the effect of the sucrose concentration alone on tracer permeability because of the effect of the solute drag phenomenon which is also operative. However, a good approximation of the effect of increased solute concentration in the condition of driver sucrose asymmetry, can be made by assuming that the flow of tracer will be a function of the mean concentration of sucrose $(\bar{C})$ and with the assumption of a linear gradient for sucrose in the membrane. Then

$$\bar{C} = \frac{C_2 + C_1}{2}. \tag{7}$$

It is possible to portray graphically the expected effect of $\bar{C}$ sucrose on tracer permeability values and this has been done with the dotted line in Fig. 3. The position of this dotted line was determined by first plotting, against sucrose concentration, the P values obtained when the sucrose was present on both sides. The dotted line was obtained by the connection of points, the location of which proceeded as follows, referring to Fig. 3. Starting at point X (0.4 M sucrose) proceed up the curve to point Y (0.2 M sucrose). Project this value for P, horizontally back to the original line indicating 0.4 M sucrose. At this point, Z, one has the theoretical value for P that illustrates the effect of viscosity created by the presence of sucrose at a mean concentration $(\bar{C})$ in the membrane. Connection of such interpolated points yields the dotted line shown in Fig. 3. The line then illustrates the effect of the presence of sucrose at $\bar{C}$ within the membrane.

Coupling of Tracer and Sucrose Flows

The present experiments were carried out to examine the coupling of hyperosmotic (driver) solute with various tracer solutes in the homopore membrane. In the experiments reported below, sucrose was used as hyperosmotic agent on side 2 at concentrations up to 1.5 M. The net volume flow was kept at zero $(J_v = 0)$ by the application of hydrostatic pressure. Tracer transmembrane permeabilities were measured under steady-state conditions for at least five, 10–20-min periods. The results shown in Table III are reported as mean P values for tracer sucrose, maltotriose, inulin, and dextran. In addition, the final line reports the unidirectional flux of sucrose (J_{suc}). This value is obtained from $P_{suc}^{2 \to 1} \times [M]_{suc}$. Interaction is considered to be positive if the permeability coefficient of the tracer down the sucrose gradient

TABLE III

COUPLING OF TRACER SOLUTE PERMEABILITY TO SUCROSE FLOW

Sucrose concentration	0	0.5	1.0	1.5
		M	*M*	*M*
Sucrose				
$P^{2 \to 1}$	2.94±0.06	1.06±0.40	1.11±0.50	1.10±0.40
$P^{1 \to 2}$	3.27±0.26	1.83±0.16	0.95±0.30	0.63±0.30
Maltotriose				
$P^{2 \to 1}$	2.19±0.07	1.25±0.12	1.06±0.23	1.42±0.12
$P^{1 \to 2}$	2.39±0.06	1.23±0.15	0.80±0.16	0.53±0.16
Inulin				
$P^{2 \to 1}$	0.45±0.01	0.41±0.06	0.47±0.12	0.61±0.04
$P^{1 \to 2}$	0.45±0.01	0.13±0.01	0.05±0.01	0.06±0.01
Dextran				
$P^{2 \to 1}$	0.55±0.02	0.43±0.06	0.53±0.12	0.55±0.07
$P^{1 \to 2}$	0.55±0.02	0.24±0.04	0.13±0.05	0.09±0.02
Sucrose Flux				
$J^{2 \to 1}$	—	0.53±0.30	1.11±0.50	1.67±0.40

P in cm s^{-1}×10^5±1 SD.

J in mol cm^{-1} s^{-2}×10^8±1 SD.

$(P_T^{2 \to 1})$ progressively increases and the corresponding $P_T^{1 \to 2}$ against the sucrose gradient decreases.

The data of Table III show an instance of little or no solute drag and two instances of positive solute drag interaction. Consider the P values for tracer sucrose on lines 1 and 2. It is seen that, except for the 1.5 M sucrose level, $P^{2 \to 1}$ and $P^{1 \to 2}$ do not significantly differ from each other indicating that tracer sucrose (mol wt 343, molecular radius 5.3 Å) does not have a molecular size adequate for interaction with driver sucrose in this membrane with 150-Å pores. Mannitol showed no flux asymmetry at any concentration of sucrose used and these values are not reported.

The trisaccharide maltotriose (mol wt 594, molecular radius 6.1 Å) shows detectable interaction at 1.0 and significant interaction at 1.5 M sucrose. Inulin (mol wt 5,000, molecular radius ~15 Å) and dextran (mol wt 17,000) show interaction at even 0.5 M sucrose. Figs. 4 and 5 present a graphic comparison of $P^{2 \to 1}$ and $P^{1 \to 2}$ values plotted againts the sucrose concentration. The lines have been drawn freehand to illustrate the relative values of the system. The maltotriose data of Table III, when plotted as in Figs. 4 and 5, show little separation of the lines until the highest concentration of sucrose is reached.

Fig. 4 for the inulin/sucrose system illustrates well the basic dogma of the solute drag concept for it suggests that tracer inulin diffusing across the membrane might be expected to show (dotted line) the decreased permeability characteristics of tracer in the presence of $\overline{C}$ sucrose. Instead, tracer inulin moving with the sucrose gradient, and thus with sucrose flow, has an increased permeability as shown by the upper line. The solute interaction

effect here has been to increase the flow of tracer inulin by the drag effect of the sucrose. Quite the opposite effect is seen when tracer inulin diffuses across the membrane against (upstream to) the sucrose flow. In this case the tracer flow is decreased by interaction with the flow of sucrose.
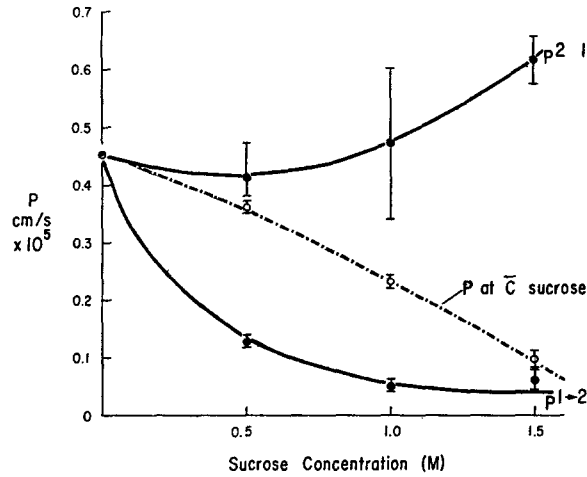

FIGURE 4. The effect of solute drag on the permeability of tracer inulin. The curve $P^{2\to1}$ is the permeability of inulin moving down the sucrose gradient and the curve $P^{1\to2}$ is inulin moving against the gradient. The dotted line represents the permeability of tracer inulin in the presence of mean concentration $(\bar{C})$ of sucrose. See text and Fig. 3 for derivation of the dotted line.
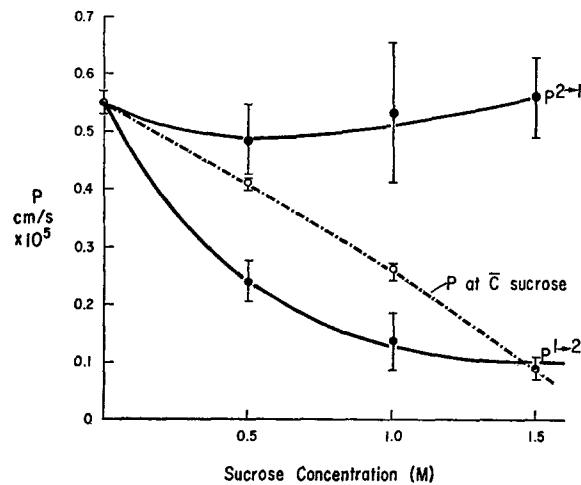

FIGURE 5. The effect of solute drag on the permeability of tracer dextran. The curve $P^{2\to1}$ is the permeability of dextran moving down the sucrose gradient and the curve $P^{1\to2}$ is dextran moving against the gradient. The dotted line represents the permeability of tracer dextran in the presence of mean concentration $(\bar{C})$ of sucrose. See text and Fig. 3 for derivation of the dotted line.

The curves shown in Fig. 5 suggest that the positive and negative effects of solute drag on tracer dextran are similar to those for inulin. The dextrans, however, are not spherical molecules such as are the other tracers used and it is even possible that the molecular characteristics of dextran in the sucrose solution (side 2) differ from those in the water (side 1). We previously (4) found it difficult to reconcile dextran data on the heteropore membranes with that of symmetric molecules.

A quantitative expression of the solute-solute interaction phenomenon is offered by the data of Table IV. Here interaction coefficients have been calculated for the various solute pairs studied. See Appendix for derivation of this term. These numbers express, in moles^{-1} cm^3, the amount of interaction between the two solutes. The parameter moles^{-1} cm^3 might be visualized as a volume (cm^3) offered for interaction per mole of solute involved.

The λ values have been calculated from the permeability coefficients cited in Table III and from data from the curves shown in Figs. 4 and 5. The single significant value cited for sucrose-sucrose reflects the high concentration required for driver sucrose to materially influence the tracer sucrose flow. The trisaccharide maltotriose shows a value of 234 at 1.0 M and 533 at 1.5 M sucrose. The values shown for inulin appear to differ but the large standard deviations listed do not warrant distinguishing individual numbers from the average of $\sim$400. The large standard deviations reported result from the propagation of errors as three numbers and their standard deviations are involved in the calculation of λ as in Eq. 11. The somewhat lower mean value of $\sim$330 shown for dextran reflects the lesser degree of interaction shown in Fig. 5.

DISCUSSION

The previous papers in this series (1–4) demonstrated that a transmembrane gradient for a permeable solute (driver solute) can influence the transmembrane movement of a second solute (tracer or driven solute). This tracer

TABLE IV

INTERACTION COEFFICIENTS (λ_{DT}) FOR SUCROSE DRIVER IN
HOMOPORE MEMBRANE 118/151

Sucrose concentration	Interaction coefficients*			
	Sucrose	Maltotriose	Inulin	Dextran
M				
0.5	<25	<25	520±46	360±41
0.75	<25	<25	405†	315†
1.0	<100	235	375±136	360±178
1.5	281	533±278	330±98	275±117

* Moles^{-1} cm^3±1 SD.
† Calculated from values obtained from Figs. 4 and 5.

solute asymmetry of flow was entitled solute drag and the phenomenon was shown to be present across frog skin (1–3), toad skin (16), and nonbiological heteroporous membranes (4). The present studies on the 150-Å radius homopore membrane also demonstrate tracer flux asymmetry under conditions of driver solute asymmetry confirming the ubiquitous nature of the solute drag process.

One of the goals of the present work has been the derivation of interaction or frictional coefficients to describe the magnitude of solute interaction. As indicated in the Appendix, equations have been developed to interrelate all the quantities within our control. With the elimination of net solvent flow ($J_v = 0$), the equation describing the flux of a neutral, permeable solute is related to tracer and driver solute concentrations, their respective permeabilities, and to the interaction of one solute with another. As developed, the interaction coefficient λ is shown to be

$$\lambda_{DT} = \frac{P_T^{2 \to 1} - P_T^{1 \to 2}}{P_D C_D} . \tag{8}$$

The interaction coefficient is a function of tracer solute flow asymmetry $(P_T^{2 \to 1} - P_T^{1 \to 2})$ as produced by the flow of driver solute $(P_D C_D)$.

The data presented here, together with that of the previous papers, indicate that a number of factors determine the degree of solute-solute interaction. These are: (a) Interaction is dependent upon the transmembrane flow of both driver and tracer solutes. If either P_T or P_D approach zero, *transmembrane interaction* becomes insignificant. This is obvious from consideration of Eq. 8 and also from review of our studies on frog skin (1, 2). In that system, raffinose as the hyperosmotic (driver) solute caused the expected effects of hyperosmolarity on skin but because of its low permeability, tracer solute asymmetry could not be demonstrated.

(b) Interaction is dependent not only upon the concentration of driver solute (Table III) but upon the permeability and the molecular size of this solute. We have shown previously (4) that as the molecular size of the driver solute increases, its effectiveness as a driver increases. This increased effectiveness, however, is mitigated by the decreased transmembrane permeability occasioned by the increased size. The tabulation of λ in Table IV is thus specific for only the indicated solute pairs in a particular membrane.

(c) Tracer solute size is also critical to the degree of interaction. As with the driver solute parameters cited above, an increase in tracer size will increase the probability of interaction with driver solute. At the same time, the increased size will limit membrane permeability. As shown before (4) with any one driver solute, the degree of asymmetry of flow of tracer was directly related to tracer size.

(d) An additional critical determinant of transmembrane solute-solute

interaction is the variable of pore size. The heteropore membrane studies (4) showed that tracer solute flow asymmetry increased when the effective pore size decreased. In the present studies, the slight interaction of mannitol-sucrose and sucrose-sucrose is held to be due to the large size of the pores (150-Å radius) compared to the size of the solutes. The larger solutes, maltotriose, inulin, and dextran, did show interaction demonstrating solute drag. These solute size-pore size relationships[2] are similar to those shown by us previously on heteropore membranes (4).

The possibility that another mechanism might contribute to asymmetric flow of solute has been considered by Patlak and Rapoport (10). Equations were derived to aid in distinguishing between the solute drag mechanism and a postulated closed circulation mechanism peculiar to heteroporous membranes. The present finding of tracer solute asymmetry on a homoporous membrane suggests that the postulated closed circulation model need not be considered as the sole mechanism for asymmetric solute flow in this system. Another version of a system with a closed circulation is that of Stender et al. (26). Their model is based upon Ussing's description of anomalous transport (27, 28). Both of these models require circulation of water. The water is pictured as arising osmotically from the side walls of cells lining intercellular ducts. Our demonstration of solute drag on noncellular, nonbiological, heteropore, and now on solid bodied homopore membranes suggests that our solute-solute interaction model is adequate to explain the phenomenon in this system. Since the nonbiological membrane findings do not differ in essence with our earlier findings on frog skin or with those of Biber and Curran (16) on toad skin, it is suggested that the

[2] Preliminary experiments have been done on a new small pored experimental membrane supplied by the Nucleopore Corporation. Characterization of the membrane is incomplete because of technical difficulties associated with diffusion through the small pores and the small total area for diffusion. The approximate pore radius given by several methods is: ~60 Å (EM), ~40 Å (Lp), 18–33 Å (P-solutes). We have selected the value of 40-Å radius, as a close approximation of the true size. A detailed description of the characteristics of this membrane will be presented in a subsequent communication. For the present study, the absolute size of these pores is not important, only that the pores are significantly smaller than 150 Å. In these preliminary studies, tracer mannitol and maltotriose were used with 1 M sucrose as driver solute. The interaction coefficients obtained are compared with those found for the 150-Å membrane (see Table IV).

Pore size	Mannitol	Maltotriose
150 Å	<25	235
40 Å	440	415

It is clear that whereas mannitol showed no significant interaction in the 150-Å membrane, it did show significant interaction when the pore size was reduced to ~40 A. Confirmation of the effectiveness of the smaller pore in promoting coupling is also seen in the increase in λ for maltotriose in the smaller pored membrane. These data substantiate our previous findings on heteropore membranes where increased solute coupling was found as the pore size was decreased.

solute drag model can adequately explain the findings in the biological systems. Recent studies of Lief and Essig with urea coupling in toad bladder (29) also support the solute drag model.

APPENDIX

The basic assumption to be made (4) regarding a single solvent with two electrically neutral solutes is:

$$J_i = \bar{C}_i(1 - \sigma_i)J_v + P_{ii}\Delta C_i + P_{ij}\Delta C_j. \qquad (1\,a)$$

Here J_i, the flux of solute i, is seen to be the resultant or summation of the effect of volume flow, diffusional flow, and solute interaction (4). In the above: $\bar{C}_i$ is the mean concentration of solute, σ_i the reflection coefficient for the solute i, J_v the volume flow across the membrane, P_{ii} the self-diffusion or self-permeability coefficient and ΔC_i the concentration gradient of solute i across the membrane. The final term in the equation represents the effect of solute interaction, P_{ij} being the cross coefficient between S_i and S_j; ΔC_j is the concentration difference of solute j across the membrane.

In the particular case of driver and tracer interaction in the present homopore study the following symbols are used: $J_D{}^{2\rightarrow1}$ and $J_T{}^{2\rightarrow1}$ represent the flow of driver D and tracer T from side 2 to side 1. $\bar{C}_D$ and $\bar{C}_T$ are the mean concentrations of D and T between sides 2 and 1. ω_D and ω_T are the respective permeabilities of D and T at zero volume flow. λ_{TD} and λ_{DT} are the cross-coupling coefficients between the two solutes. $C_{D2} - C_{D1}$ and $C_{T2} - C_{T1}$ are the concentration differences of D and T across the membrane and R and T have their usual meaning being the ideal gas constant and absolute temperature, respectively.

The directional movement of the two solutes in the present system may be represented as:

$$J_D{}^{2\rightarrow1} = \bar{C}_D(1 - \sigma_D)J_v{}^{2\rightarrow1} + \omega_D RT(C_{D2} - C_{D1}) + \lambda_{TD}\bar{C}_D J_T{}^{2\rightarrow1}, \qquad (2\,a)$$

$$J_T{}^{2\rightarrow1} = \bar{C}_T(1 - \sigma_T)J_v{}^{2\rightarrow1} + \omega_T RT(C_{T2} - C_{T1}) + \lambda_{DT}\bar{C}_T J_D{}^{2\rightarrow1} \qquad (3\,a)$$

where the third term in Eqs. 2a and 3a is modified from the general expression in Eq. 1a.

This form of representing solute movement is particularly suitable to show effects of the mutual interaction between two solutes. The last term on the right side describes the process in which the flux of one solute acts on the other solute which has a certain average concentration in the interaction region. This interaction is described by the coefficient λ. In the case where the solute drag contribution to the flux is linear in $\bar{C}$ and J, λ should be a constant which characterizes the interaction. Values of λ have the units of $cm^3\ mol^{-1}$. The physical meaning of λ may be described as the reciprocal of the $\bar{C}_T$ required to produce a unit tracer flux for each unit of driver flux. The reciprocal parameter then has the dimension of mole cm^{-3}. λ here has a connotation somewhat similar to the "cross section" concept of nuclear physics.

In the reported experiments the potential osmotic flow occasioned by the presence

of D on side 2 was countered by hydrostatic pressure so that $J_v = 0$. As a result, the first term in each of the Eqs. 2 a and 3 a will drop out. Because of the very low concentration of T on side 2, the final term in Eq. 2 a will be insignificant so that the flow of driver solute is only concentration and diffusion dependent and becomes

$$J_D^{2 \to 1} = \omega_D RT(C_{D2} - C_{D1}), \tag{4 a}$$

and the flow of tracer becomes

$$J_T^{2 \to 1} = \omega_T RT(C_{T2} - C_{T1}) + \lambda_{DT}\bar{C}_T J_D^{2 \to 1}. \tag{5 a}$$

Substituting 4 a into 5 a we obtain:

$$J_T^{2 \to 1} = \omega_T RT(C_{T2} - C_{T1}) + \lambda_{DT}\bar{C}_T \omega_D RT(C_{D2} - C_{D1}). \tag{6 a}$$

When driver solute is present in an appreciable concentration on only side 2, $C_{D1} = 0$ and $C_{D2} = C_D$. Likewise for tracer solute present only on side 2, $C_{T1} = 0$ and $C_{T2} = C_T$.

The equation for unidirectional tracer flow can now be written:

$$J_T^{2 \to 1} = \omega_T RTC_T + \lambda_{DT}\bar{C}_T \omega_D RTC_D. \tag{7 a}$$

Similarly, for the flow of tracer against the flux of the driver $(J_T^{1 \to 2})$ is expressed by:

$$J_T^{1 \to 2} = \omega_T RTC_T - \lambda_{DT}\bar{C}_T \omega_D RTC_D, \tag{8 a}$$

where $C_{T2} = 0$, $C_{T1} = C_T$ and $C_{D1} = 0$, and $C_{D2} = C_D$.

Thus, under the conditions of our experiments the net flow will be described by

$$J_T = J_T^{2 \to 1} - J_T^{1 \to 2} = \lambda_{DT}C_T \omega_D RTC_D, \tag{9 a}$$

where $\bar{C}_T = C_{T1} + C_{T2}/2$ as defined by Katchalsky and Curran (24).

From Eq. 9 a we may define the coefficient of interaction in this system as:

$$\lambda_{DT} = \frac{J_T^{2 \to 1} - J_T^{1 \to 2}}{C_T \omega_D RTC_D} \tag{10 a}$$

Eq. 10 a permits calculation of λ from flux data and permeability measurements. In practice, λ may be calculated from permeability coefficients as:

$$\lambda_{DT} = \frac{P_T^{2 \to 1} - P_T^{1 \to 2}}{P_D C_D}, \tag{11 a}$$

for $J_T/C_T = P_T$ and $\omega_D RT = P_D$.

REFERENCES

1. FRANZ, T. J., and J. T. VAN BRUGGEN. 1967. A possible mechanism of action of DMSO. *Ann. N.Y. Acad. Sci.* **141:**302.
2. FRANZ, T. J., and J. T. VAN BRUGGEN. 1967. Hyperosmolarity and the net transport of nonelectrolytes in frog skin. *J. Gen. Physiol.* **50:**933.
3. FRANZ, T. J., W. R. GALEY, and J. T. VAN BRUGGEN. 1968. Further observations on asymmetrical solute movement across membranes. *J. Gen. Physiol.* **51:**1.
4. GALEY, W. R., and J. T. VAN BRUGGEN. 1970. The coupling of solute fluxes in membranes. *J. Gen. Physiol.* **55:**220.
5. ALLBRIGHT, J. G., and R. MILLS. 1965. A study of diffusion in the ternary system, labeled urea-urea-water, at 25° by measurement of the intradiffusion coefficients of urea. *J. Phys. Chem.* **69:**3120.
6. ELLERTON, H. D., and P. J. DUNLOP. 1967. Diffusion and frictional coefficients for four compositions of the system water-sucrose-mannitol at 25°. *J. Phys. Chem.* **71:**1291.
7. DUNLOP, P. J. 1957. Interacting flows in diffusion of the system raffinose-urea-water. *J. Phys. Chem.* **61:**1619.
8. GOLDSTEIN, D. A., and A. K. SOLOMON. 1960. Determination of equivalent pore radius for human red cells by osmotic pressure measurement. *J. Gen. Physiol.* **44:**1.
9. PAGANELLI, C. V., and A. K. SOLOMON. 1957. The rate of exchange of tritiated water across the human red cell membrane. *J. Gen. Physiol.* **41:**259.
10. PATLAK, C. S., and S. I. RAPOPORT. 1971. Theoretical analysis of net tracer flux due to volume circulation in a membrane with pores of different sizes. Relation to solute drag model. *J. Gen. Physiol.* **57:**113.
11. KEDEM, O., and A. KATCHALSKY. 1958. Thermodynamic analysis of the permeability of biological membranes to non-electrolytes. *Biochim. Biophys. Acta.* **27:**229.
12. KEDEM, O., and A. KATCHALSKY. 1961. A physical interpretation of the phenomenological coefficients of membrane permeability. *J. Gen. Physiol.* **45:**143.
13. KEDEM, O., and A. KATCHALSKY. 1963. Permeability of composite membranes. *Trans. Faraday Soc.* **59:**1918.
14. KEDEM, O., and A. ESSIG. 1965. Isotope flows and flux ratios in biological membranes. *J. Gen. Physiol.* **48:**1047.
15. HOSHIKO, T., and B. D. LINDLEY. 1967. Phenomenological description of active transport of salt and water. *J. Gen. Physiol.* **50:**729.
16. BIBER, T. U. L., and P. F. CURRAN. 1968. Coupled solute fluxes in toad skin. *J. Gen. Physiol.* **51:**606.
17. PRICE, P. B., and R. M. WALKER. 1962. Electron microscope observation of etched tracks from spallation recoils in mica. *Phys. Rev. Lett.* **8:**217.
18. PRICE, P. B., and R. M. WALKER. 1962. Chemical etching of charged-particle tracks in solids. *J. Appl. Phys.* **33:**3407.
19. FLEISCHER, R. L., P. B. PRICE, R. M. WALKER, and E. L. HUBBARD. 1964. Track registration in various solid-state nuclear track detectors. *Phys. Rev.* **133:**A1443.
20. BEAN, C. P., M. V. DOYLE, and G. ENTINE. 1970. Etching of submicron pores in irradiated mica. *J. Appl. Phys.* **41:**1454.
21. BECK, R. E., and J. S. SCHULTZ. 1972. Hindrance of solute diffusion within membranes as measured with microporous membranes of known pore geometry. *Biochim. Biophys. Acta.* **255:**273.
22. QUINN, J. A., J. L. ANDERSON, W. S. HO, and W. J. PETZNY. 1972. Model pores of molecular dimension. *Biophys. J.* **12:**990.

23. GINZBURG, B. Z., and A. KATCHALSKY. 1963. The frictional coefficients of the flows of nonelectrolyte through artificial membranes. *J. Gen. Physiol.* **47**:403.

24. KATCHALSKY, A., and P. F. CURRAN. 1965. Nonequilibrium Thermodynamics in Biophysics. Harvard University Press, Cambridge, Mass., p. 72.

25. CURRAN, P. F., A. E. TAYLOR, and A. K. SOLOMON. 1967. Tracer diffusion and unidirectional fluxes. *Biophys. J.* **7**:879.

26. STENDER, S., K. KRISTENSEN, and E. SKADHAUGE. 1973. Solvent drag by solute-linked water flow. *J. Membrane Biol.* **11**:377.

27. USSING, H. H. 1966. Anomalous transport of electrolytes and sucrose through the isolated frog skin induced by hypertoxicity of the outside bathing solution. *Ann. N.Y. Acad. Sci.* **137**:543.

28. USSING, H. H., and B. JOHANSEN. 1969. Anomolous transport of sucrose and urea in toad skin. *Nephron.* **6**:317.

29. LIEF, P. D., and A. ESSIG. 1973. Urea transport in the toad bladder; coupling of urea flows. *J. Membrane Biol.* **12**:159.